Quaternary Research 78 (2012) 275–284

Contents lists available at SciVerse ScienceDirect

Quaternary Research

journal homepage: www.elsevier.com/locate/yqres

Holocene hydro-climatic change and effects on carbon accumulation inferred from a peat bog in the Attawapiskat River watershed, Hudson Bay Lowlands, Canada

Joan Bunbury [a,*], Sarah A. Finkelstein [a], Jörg Bollmann [b]

[a] Department of Geography, University of Toronto, 100 St. George Street, Toronto, Ontario, Canada M5S 3G3
[b] Department of Geology, University of Toronto, 22 Russell Street, Toronto, Ontario, Canada, M5S 3B1

ARTICLE INFO

Article history:
Received 15 February 2012
Available online 16 June 2012

Keywords:
Paleohydrology
Paleoecology
Quantitative reconstructions
Northern peatlands
Medieval Climate Anomaly

ABSTRACT

Multiple proxies from a 319-cm peat core collected from the Hudson Bay Lowlands, northern Ontario, Canada were analyzed to determine how carbon accumulation has varied as a function of paleohydrology and paleoclimate. Testate amoeba assemblages, analysis of peat composition and humification, and a pollen record from a nearby lake suggest that isostatic rebound and climate may have influenced peatland growth and carbon dynamics over the past 6700 cal yr BP. Long-term apparent rates of carbon accumulation ranged between 8.1 and 36.7 g C m^{-2} yr^{-1} (average = 18.9 g C m^{-2} yr^{-1}). The highest carbon accumulation estimates were recorded prior to 5400 cal yr BP when a fen existed at this site, however following the fen-to-bog transition carbon accumulation stabilized. Carbon accumulation remained relatively constant through the Neoglacial period after 2400 cal yr BP when pollen-based paleoclimate reconstructions from a nearby lake (McAndrews et al., 1982) and reconstructions of the depth to the water table derived from testate amoeba data suggest a wetter climate. More carbon accumulated per unit time between 1000 and 600 cal yr BP, coinciding in part with the Medieval Climate Anomaly.

Introduction

The Hudson Bay Lowlands (HBL) forms the second largest cold-climate peatland in the world covering ~325,000 km^2 in northern Canada (Martini, 2006). The poorly decomposed plant material accumulating in these waterlogged northern peatlands is both a carbon pool and annual carbon sink of global significance, exerting a cooling effect on the climate (Frolking and Roulet, 2007). By contrast, the emission of methane (CH_4) through anaerobic metabolism in peat-forming wetlands enhances the greenhouse effect. Climate–carbon models thus need to parameterize the carbon balance of peatland ecosystems correctly in order to model changing Earth systems accurately (Kleinen et al., 2010; Wania et al., 2009).

Although the size of the carbon pool in Ontario's HBL has not been systematically measured, it is estimated to be on the order of 26 billion tonnes (Far North Science Advisory Panel, 2010). Northern peatlands in general are critical to understanding biosphere–climate interactions (Beilman et al., 2009; Gorham, 1991), and the HBL in particular is highly significant in this regard due to its vast size. Despite the importance of these systems to the global carbon cycle and the climate, uncertainty remains concerning the controls on the carbon balance in northern peatlands (Frolking and Roulet, 2007). Specifically, more information is needed on the response of peatlands to changes in air temperature and moisture balance, and on the effects of autogenically driven successional changes on carbon balance.

During the post-glacial period, climate changes influenced peatland vegetation and carbon dynamics. For example, Yu et al. (2010) reported that the greatest rates of carbon accumulation occurred in response to high summer insolation and strong seasonality during the early Holocene. Additional paleoecological studies linking past rates of carbon accumulation and changes in temperature and moisture regimes will improve our ability to quantify this relationship. The paleoecological record provides an opportunity to measure the relationships between past changes in carbon accumulation, temperature and surface moisture balance, as well as to consider the role of local factors such as topographic controls and autogenically driven changes (MacDonald et al., 2006; Yu et al., 2003, 2010). The study of paleo-records from HBL peatlands is particularly urgent because the region is likely to experience amplified climate warming relative to other regions in Canada and the world, in part due to feedbacks associated with declines in sea-ice extent in Hudson Bay and resulting decrease in surface albedo (Gagnon and Gough, 2005).

The objective of our study is to use multiple proxies in a peat core from a bog in the Attawapiskat River watershed in the western James Bay region of the HBL to measure broad-scale changes in rates of carbon accumulation during the Holocene, and to evaluate the potential role of hydro-climatic conditions in controlling those rates. Testate amoebae (Protozoa: Rhizopoda) are indicator organisms that can be used to assess these conditions as they respond quickly to changes in surface moisture conditions. They are abundant in *Sphagnum* peatlands

* Corresponding author. Fax: +1 416 946 3886.
E-mail addresses: bunburyj@geog.utoronto.ca (J. Bunbury), finkelstein@geog.utoronto.ca (S.A. Finkelstein), bollmann@geology.utoronto.ca (J. Bollmann).

0033-5894/$ – see front matter
doi:10.1016/j.yqres.2012.05.013

and have a test that preserves well in peat deposits, making them effective paleohydrological indicators (Charman, 2001).

Surface moisture conditions, quantified by depth to water-table (DWT) estimates based on testate amoebae assemblages, will be complemented by measurements of the degree of peat humification, which is a second method to estimate fluctuations in hydro-climate (de Jong et al., 2010). Warmer and/or drier conditions can lower the water-table, increasing microbial activity under aerobic conditions and therefore the rate of peat decomposition and release of humic acids which can be measured spectrophotometrically following alkali extraction (Blackford and Chambers, 1993). While values of peat humification estimated by this method are highly sensitive to contributing vegetation type (Yeloff and Mauquoy, 2006), these measurements can be used to estimate the relative degree of peat decomposition through sections of the core with peat of uniform composition, and when taken alongside other proxies, can provide supporting evidence for changes in water-table position (e.g. Loisel and Garneau, 2010).

Finally, we make use of regional pollen records to provide independent assessments of paleoclimatic change, for comparison with calculated rates of carbon accumulation. Although regional paleoclimate records from the HBL are scarce, a pollen record spanning the past ~8600 yr from R Lake on the Sutton Ridges (Fig. 1; McAndrews et al., 1982) and multi-proxy records (including macrofossils, pollen, testate amoebae, and geochemistry) from three peat bogs in the southern James Bay region (Fig. 1; Kettles et al., 2000) can be used to draw some basic inferences on Holocene paleoclimate, notwithstanding the low sampling resolution in those studies. Taken together, these records suggest a mid-Holocene warm period after 6500 cal yr BP, followed by Neoglacial cooling after 2500 cal yr BP, which McAndrews et al. (1982) suggested may have led to regional paludification. In addition to qualitative inferences based on the diagrams presented in the above studies, we also present new quantitative pollen-inferred temperature and precipitation reconstructions from the record of McAndrews et al. (1982) using the modern pollen database of Whitmore et al. (2005) and the modern analogue technique to provide an independent record of Holocene climate history for the interpretation of peatland dynamics in our study region. Testate amoeba records, peat humification measurements, and regional pollen reconstructions will be used to evaluate the potential effects of hydro-climatic change on Holocene carbon accumulation in the HBL.

Study area

Following the retreat of the Laurentide Ice Sheet from the HBL region about 8500 cal yr BP, the Tyrrell Sea inundated this low-relief region (Dyke and Prest, 1987). Isostatic rebound since that time resulted in the emergence of an extensive lowland landscape, mantled in impermeable marine deposits, upon which peatlands have developed. Roughly 90% of the landscape in the HBL is covered by a mosaic of peatland types including open and treed bogs, rich, intermediate and poor fens, as well as marshes and areas of open water (Martini, 2006; Riley, 2003, 2011). Our study site is located in the Attawapiskat River watershed of the central HBL in northeastern Ontario (Fig. 1). The peat core analyzed in this study was collected from a shrub bog with a hummock and hollow structure (52.71°N, 84.18°W, 104 masl) located approximately 90 km upriver from the community of Attawapiskat. The collection site is underlain by Paleozoic sedimentary bedrock overlain by marine sediments (Fulton, 1995; Wheeler et al., 1997). Hudson Bay exerts a strong cooling effect on the HBL region, even well inland from the coast. Mean January

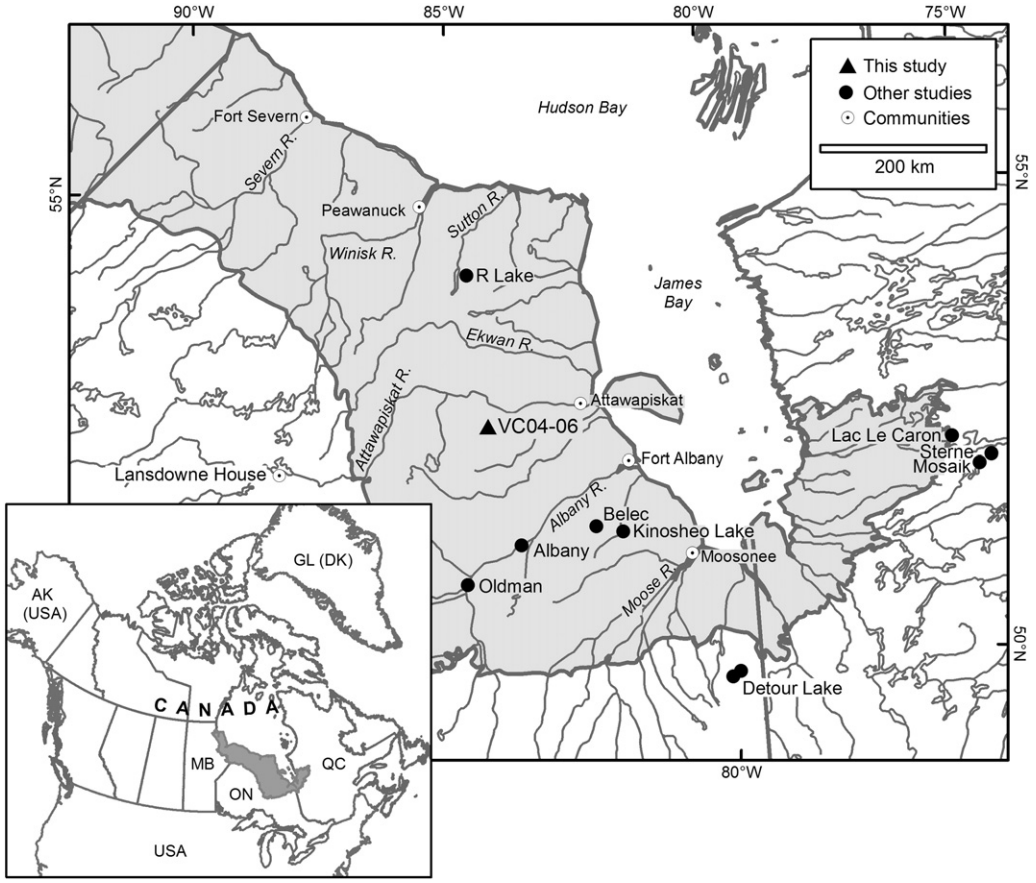

Figure 1. Location map of the VC04-06 peat core collected from the Attawapiskat River watershed, Hudson Bay Lowlands, northern Ontario, Canada. Sites of other studies are indicated and include R Lake (McAndrews et al., 1982), Oldman, Albany, and Belec bogs (Glaser et al., 2004), Kinosheo Lake and Detour Lake bogs (Kettles et al., 2000), and Eastmain region peatlands (Loisel and Garneau, 2010; van Bellen et al., 2011a,b).

https://doi.org/10.1016/j.yqres.2012.05.013 Published online by Cambridge University Press

and July temperatures at the closest inland weather station, Lansdowne House (200 km west of the study site), are −22.3°C and 17.2°C, respectively and mean annual air temperatures are below freezing (−1.3°C; Environment Canada, 2000), allowing for the development of sporadic discontinuous permafrost (National Atlas Information Service, 1995). The region receives ~700 mm of precipitation annually, with snowfall potential in all months but July and August. The core was taken in a hollow, where surface vegetation consisted of *Sphagnum fuscum* and *Cladonia* spp., with occurrences of the herbaceous plants *Eriophorum vaginatum*, *Rubus chamaemorus*, *Scirpus caespitosus*, and *Carex* spp. in the immediate vicinity. Trees were scarce, shrubs were more abundant, and taxa encountered included *Picea mariana*, *Larix laricina*, *Chamaedaphne calyculata*, and *Kalmia angustifolia*.

Methods

Field and laboratory methods

A 319-cm peat core (core VC04-06) was recovered from a bog in the Attawapiskat River basin in July 2009 using Jeglum (depths 0–82 cm; 8 × 8 cm box) and Russian (depths 82–319 cm; 5 cm diameter barrel) peat corers. The upper 304 cm of the core was comprised of peat and the lower 15 cm was marine clay. The core chronology was determined through a combination of lead-210 (^{210}Pb) and accelerator mass spectrometry (AMS) radiocarbon dating (^{14}C) methods. Dried samples for ^{210}Pb dating were sent to Flett Research Ltd. (Winnipeg, Manitoba) for analysis by alpha spectrometry and a constant rate of supply (CRS) model was applied to the ^{210}Pb values. Six ^{14}C dates were measured at Beta Analytic (Miami, Florida) on hand-picked macrofossils (i.e. *Sphagnum* stems, wood, twigs, and conifer needles) and an age-depth model was developed using the clam package ("classical" age-depth modeling; Blaauw, 2010) in R (R Development Core Team, 2011). Conventional ^{14}C ages were calibrated to 'calendar' years in clam using the IntCal09 calibration dataset (Reimer et al., 2009) and an age-depth model was developed using linear interpolation between the "best" age estimates derived from 1000 iterations (see Blaauw, 2010 for further details). Dates are reported as calendar years before present (cal yr BP) where 0 = AD 1950.

One cm^3 of peat was sub-sampled about every 2.5 cm and dried to constant mass at 105°C to measure bulk density, percent carbon (C) and nitrogen (N). Ground peat samples for C and N were analyzed on an ESC 4010 Elemental Combustion System for CHNS-O (configured for C and N; Costech Analytical Technologies, Valencia, CA). Either one or two replicates run on each batch were used to assess within-batch errors, which were then averaged across all batches and used as the measurement error for C and N. C mass was determined by multiplying percent C by bulk density, and long-term apparent rate of C accumulation (LORCA) was calculated by multiplying C mass by the peat accumulation rates based on the age-depth model.

A 2-cm^3 sub-sample of peat was taken at either every 5 or 10 cm in the core for testate amoeba analysis for a total of 52 samples that were soaked overnight, boiled gently in distilled water and sieved, retaining the size fraction between 10 and 350 μm (Charman et al., 2000). At least 100 testate amoebae were identified (Payne and Mitchell, 2009) from each of the 52 levels under 400× magnification and taxonomy followed Booth (2008) with reference to Charman et al. (2000). *Nebela tincta* type and *Nebela parvula* type indicate comparable ecological conditions (Charman et al., 2000), therefore we grouped them into *Nebela tincta-parvula* type as we could not always confidently differentiate between the two. The rotifer *Habrotrocha angusticollis* was included in the total testate amoeba counts, and all taxa were presented as percent abundance using the software C2 (Juggins, 2003).

A detrended correspondence analysis (DCA) was performed on a data matrix of 43 square-root transformed taxa from 52 levels with down-weighting of rare species using CANOCO v 4.5 (ter Braak and Šmilauer, 2002). Statistically significant stratigraphic zones were defined from the testate amoeba data using constrained cluster analysis (CONISS; Grimm, 1987) and a broken-stick model (Bennett, 1996) in the rioja package in R (Juggins, 2009; R Development Core Team, 2011). A weighted-averaging (WA) transfer function developed by Booth (2008) was applied to the testate amoeba assemblages to reconstruct past depths to water-table (DWT) using the software package C2 (Juggins, 2003). *Cyclopyxis arcelloides* type, *Phryganella acropodia* type and *Difflugia globulosa* type were grouped together for the DWT reconstruction due to the presence of intermediate morphologies and to harmonize the taxonomy of our fossil data with the calibration set. Sample-specific standard errors and model performance statistics were generated using bootstrap simulations (1000 iterations; see Booth, 2008 for further details).

Subsamples of peat for humification analysis were taken every 5 cm in the peat core and corresponded with the testate amoeba levels. Extraction of humic acids was performed using the standard NaOH technique with absorption measurements made at 540 nm (Blackford and Chambers, 1993). Replicates were run on each batch to assess within-batch errors, which were then averaged across all batches and used as the measurement error. Duplicate measurements were taken on each sample and the average absorbance values were detrended using linear regression to account for the long-term decay trend present in peat sequences (Charman, 2002); the regression residuals have been plotted as the absorbance values. Higher percent absorbance indicates more humified peat, whereas lower percentages reveal the opposite.

We calculated mean summer air paleo-temperature (TJJA) and total annual paleo-precipitation (ANNP) since 6700 cal yr BP using the fossil pollen record from R Lake located in the Sutton Ridges (54.3°N, 84.6°W, 142 masl; McAndrews et al., 1982) and the North American Modern Pollen Database (Whitmore et al., 2005). The fossil record was extracted from the Neotoma Paleoecology Database and taxa present in <0.5% abundance were considered rare and removed from the analysis. Sites in the modern database with pollen sums <300 grains were excluded. Climatic variables were estimated by combining 21 fossil pollen taxa from 36 levels and 1983 modern pollen assemblages from lake environments using the Modern Analogue Technique (MAT), with a squared chord distance (SCD) dissimilarity metric to assess differences between the fossil and modern assemblages (Overpeck et al., 1985) in the computer program C2 (Juggins, 2003). Temperature and precipitation estimates presented here are the averages of the top three analogues (Williams and Shuman, 2008), and bootstrap cross-validation (500 iterations) was used to assess model performance.

Results

Core description, chronology, and peat accumulation

The boundary between the acrotelm and the catotelm in the peat core was observed at a depth of 33 cm based on peat bulk density

Table 1
^{210}Pb dates (at bottom of sediment section) from peat core VC04-06, Hudson Bay Lowlands, northern Ontario computed using a constant rate of supply (CRS) model.

Interval (cm)	^{210}Pb total activity (DPM/g)	Years before AD 2009
0–1	70.21	18.5
1–2	43.07	36.1
2–3	32.93	59.1
3–4	14.38	75.7
4–5	10.30	92.9
5–6	5.09	104.4
6–7	3.50	
7–8	2.22	
10–11	2.80	
12–13	2.37	
15–16	1.67	

https://doi.org/10.1016/j.yqres.2012.05.013 Published online by Cambridge University Press

Table 2
Radiocarbon (^{14}C) dates from peat core VC04-06, Hudson Bay Lowlands, northern Ontario.

Lab code	Interval (cm)	Conventional ^{14}C	2-sigma calibrated age range (cal yr BP)	*Clam* best estimate (cal yr BP)	δ^{13}C	Material
Beta-281000	62–63	1130 ± 40	959–1145	1037	−26.1	*Sphagnum* stems
Beta-281001	110–111	2140 ± 40	2000–2183	2140	−27.7	Twigs
Beta-281002	185–186	3770 ± 40	4064–4248	4138	−27.1	*Sphagnum* stems
Beta-280032	237–238.5	4760 ± 40	5450–5589	5488	−26.6	Wood
Beta-281003	303–304	5820 ± 40	6530–6730	6667	−26.2	Wood fragments
Beta-281004	303–304	5890 ± 40	6635–6797	6667	−28.9	Conifer needles

(Fig. 3). The peat section overlaid light gray marine clay, with a distinct peat/mineral contact at a depth of 304 cm. We combined ^{210}Pb and ^{14}C dating to develop the core chronology. The activity of ^{210}Pb declined regularly (Table 1), allowing for the application of the CRS model and the inference of ages. Background concentrations (supported ^{210}Pb) were reached at a depth of 6 cm, which was somewhat higher in the core relative to other northern peatland sites (e.g. Ali et al., 2008), suggesting the possibility of lower rates of recent peat accumulation, although data from more cores are required to corroborate that idea. The age model built from both the ^{210}Pb and the ^{14}C dates indicates a relatively constant rate of peat accumulation since 6700 cal yr BP (mean = 0.047 cm yr^{-1}) with peat accumulating somewhat more slowly between 5500 and 1000 cal yr BP (Tables 1 and 2, Fig. 2), although the use of just six radiocarbon dates limits the possibility for detailed discussion of changes in the rates of peat accumulation.

Bulk density, percent carbon, percent nitrogen, C/N, and carbon accumulation

Bulk density values exhibited a long-term decrease from the bottom to the top of the core, ranging from 0.14 gm/cm^3 at the base, to the lowest value of 0.03 gm/cm^3 in the acrotelm (mean of entire core = 0.09 gm/cm^3). Carbon (C) values ranged from 45 to 50% of dry mass up to ~1900 cal yr BP, and between 40 and 45% thereafter (mean of core = 46%). Nitrogen (N) values ranged between 1 and 3% of dry mass and were generally higher (>2%) until ~5100 cal yr BP, then exhibited a gradual decline up to the present (mean = 1.2%). The ratios of C to N increased and became more variable through time, with values below 30 up to ~5100 cal yr BP, between 30 and 80 up to ~1700 cal yr BP, and as high as 159 thereafter (mean = 58). A period of declining and/or lower ratios occurred from ~1050 to 550 cal yr BP and again during the most recent 100 yr. Long-term apparent rates of C accumulation (LORCA) ranged between 20 and 40 g C m^{-2} yr^{-1} (mean ± SD = 30.7 ± 3.6 g C m^{-2} yr^{-1}) up to 5500 cal yr BP, then exhibited a subtle, long-term decrease, with higher C accumulation (up to 26 g C m^{-2} yr^{-1}; mean ± SD = 20.6 ± 4.2 g C m^{-2} yr^{-1}) between 1000 and 600 cal yr BP, followed by lower values (8 to 15 g C m^{-2} yr^{-1}; mean ± SD = 9.8 ± 1.1 g C m^{-2} yr^{-1}) from 600 to 300 cal yr BP, and variable estimates thereafter (Fig. 3).

Testate amoebae and peat humification

Of the 43 taxa (42 testate amoebae and the rotifer *Habrotrocha angusticolis*) encountered in the core, 12 had ≥25 occurrences and five taxa had >45% abundance in a given sample (Table 3; Figs. 4 and 5). A detrended correspondence analysis (DCA) revealed a gradient length of 3.0 standard deviation units indicating that the

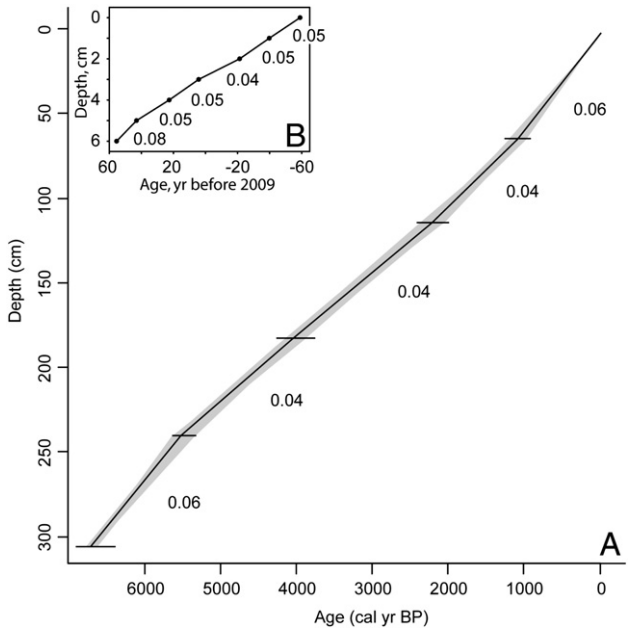

Figure 2. Chronology for the VC04-06 peat core collected from the Hudson Bay Lowlands, northern Ontario, Canada; A. The entire chronology combining ^{210}Pb and ^{14}C dates (filled circles, Tables 1 and 2), and B. The ^{210}Pb dates (Table 1). Peat accumulation rates (cm yr^{-1}) are indicated on the graphs.

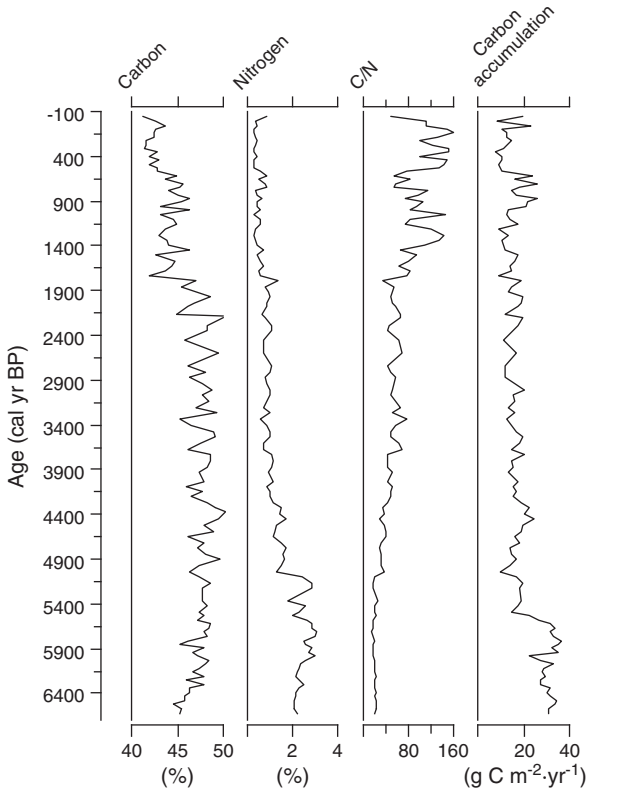

Figure 3. Bulk density, percent carbon, percent nitrogen, carbon-nitrogen ratio (C/N), and carbon accumulation estimates from core VC04-06, Hudson Bay Lowlands, northern Ontario, Canada. The dashed line separates the acrotelm (above) from the catotelm (below).

https://doi.org/10.1016/j.yqres.2012.05.013 Published online by Cambridge University Press

turnover in the testate amoeba community over the post-glacial period was relatively high (ter Braak and Šmilauer, 2002), and about one-third of the variance in the organism data was explained by the first two DCA axes (1 = 22.4%; 2 = 9.5%; Fig. 6). Samples from zone 1 are clustered on the right side of axis 1, and do not overlap with samples dating to post-4500 cal yr BP. Zone 2 and 3 samples overlap on the left side of axis 1, whereas samples from zone 4 are clustered primarily in the bottom left-hand corner of the plot. Stratigraphic zones delineated based on the testate amoeba assemblages are used to discuss changes in the DCA axis scores as well as the depth to water-table (DWT) reconstructions and peat humification; four significant zones resulted from the cluster analysis and the broken stick method (Bennett, 1996; Grimm, 1987). Testate amoeba-inferred DWT were below ground surface throughout the record, with the majority of the values 20 cm or less (min = 1.2 cm, max = 38.4 cm, median = 7.2 cm). Sample-specific standard errors range between 9.4 cm and 11.8 cm per sample, with an average standard error of 9.8 cm.

Zone 1 — 6600 to 4500 cal yr BP

The aquatic species *Centropyxis aculeata* type dominated (up to 55% of the assemblages) this zone, with *Centropyxis cassis* type, *Cyclopyxis arcelloides* type, *Phryganella acropodia* type, and *Habrotrocha angusticollis*. *Archerella flavum*, *Hyalosphenia elegans*, *Hyalosphenia papilio*, *Heleopera sphagni* and *Assulina muscorum* were only present or present in greater abundance prior to 5800 cal yr BP. *Nebela collaris-bohemica* type reached its maximum abundance in this zone. Peat humification values were initially higher then declined by 5900 cal yr BP and remained consistently low through the rest of the zone. Sample scores on DCA axis 1 were high, and scores on axis 2 were constant over the 1700-yr period. Testate amoeba-inferred DWT declined throughout this zone indicating shallow water-table depths (~1–10 cm), with an average error of ±9.5 cm. We recognize, however, that our estimates may be less reliable here due to the dominance of minerotrophic taxa that are not well represented in the modern training set (Booth, 2008).

Zone 2 — 4500 to 2400 cal yr BP

The onset of this zone is marked by the abrupt decline of several taxa, including *Centropyxis* spp., *C. arcelloides* and *P. acropodia*, and a rapid increase in *Difflugia pulex* and *A. flavum*. *Difflugia pristis* type, *Heleopera sphagni*, *H. angusticollis*, and *Arcella catinus* type are other important taxa in this zone. Sample scores on DCA axis 1 declined, whereas those on DCA axis 2 increased, and peat humification values increased initially and then remained stable following ~3900 cal yr BP. DWT values increased from ~1 to 15.5 cm (±10.4 cm within the zone) and declined to ~9 cm by 2400 cal yr BP.

Table 3
Names, authorities, number of samples (out of 52) in which the taxon occurred (N), and maximum and mean abundance in any one sample (%) for testate amoeba taxa presented in Figure 4 from core VC04-06, Hudson Bay Lowlands, northern Ontario, Canada.

	Taxon	Authority	N	Max	Mean
1	*Archerella flavum*	(Archer) Penard	49	84.4	25.2
2	*Heleopera sphagni*	(Leidy) Cash and Hopkinson	39	25.5	4.9
3	*Difflugia pulex*	Penard	38	67.6	16.3
4	*Habrotrocha angusticollis*	Murray	35	22.2	4.2
5	*Arcella discoides* type	Ehrenberg	34	50.5	4.1
6	*Difflugia pristis* type	Penard	34	55.3	5.6
7	*Assulina muscorum*	Greef	34	24.0	2.9
8	*Arcella catinus* type	Penard	30	24.4	2.6
9	*Trigonopyxis arcula* type	(Leidy) Penard	28	10.0	1.4
10	*Phryganella acropodia* type	(Hertwig and Lesser) Cash and Hopkinson	27	24.8	2.7
11	*Hyalosphenia papilio*	Leidy	26	48.0	3.6
12	*Hyalosphenia elegans*	Leidy	25	22.0	2.7
13	*Pseudodifflugia fulva* type	(Archer) Penard	22	10.0	1.5
14	*Centropyxis aculeata* type	(Ehrenberg) von Stein	17	55.6	7.9
15	*Bullinularia indica*	Penard	16	13.0	0.9
16	*Assulina seminulum*	(Ehrenberg) Leidy	15	19.4	0.9
17	*Trigonopyxis minuta* type	Schönborn and Peschke	15	3.0	0.4
18	*Arcella artocrea*	Leidy	14	2.1	0.3
19	*Nebela militaris* type	Penard	14	17.5	1.8
20	*Nebela tincta-parvula* type	(Leidy) Awerintzew; Cash and Hopkinson	14	8.5	0.8
21	*Centropyxis cassis* type	(Wallich) Deflandre	13	18.9	2.3
22	*Heleopera petricola*	Leidy	13	12.0	0.7
23	*Amphitrema wrightianum*	Archer	12	18.8	0.8
24	*Difflugia globulosa* type	Dujardin	11	8.3	0.6
25	*Heleopera sylvatica*	Penard	11	12.9	0.8
26	*Cyclopyxis arcelloides* type	(Penard) Deflandre	9	17.8	1.5
27	*Hyalosphenia subflava*	Cash and Hopkinson	8	3.0	0.2
28	*Nebela collaris-bohemica* type	Taranek	8	7.0	0.4
29	*Difflugia lucida* type	Penard	7	11.8	0.5
30	*Trinema-Corythion* type	Refer to Booth (2008)	7	2.9	0.2
31	*Hyalosphenia minuta*	Cash	6	9.3	0.4
32	*Euglypha tuberculata* type	Dujardin	5	6.0	0.3
33	*Centropyxis platystoma* type	(Penard) Deflandre	4	7.1	0.2
34	*Pseudodifflugia fasicularis*	Penard	4	4.0	0.2
35	*Euglypha rotunda* type	Wailes and Penard	2	12.6	0.3
36	*Cryptodifflugia sacculus*	Penard	1	1.7	0.03
37	*Difflugia leidyi*	Wailes	1	1.0	0.02
38	*Difflugia rubescens*	Penard	1	0.9	0.02
39	*Euglypha strigosa*	(Ehrenberg) Leidy	1	2.0	0.04
40	*Lesquereusia modesta*	Schlumberger	1	1.0	0.02
41	*Lesquereusia spiralis*	Schlumberger	1	1.0	0.02
42	*Nebela vitraea* type	Penard	1	2.0	0.04
43	*Quadrulella symmetrica*	(Wallich) Schulze	1	1.0	0.02

https://doi.org/10.1016/j.yqres.2012.05.013 Published online by Cambridge University Press

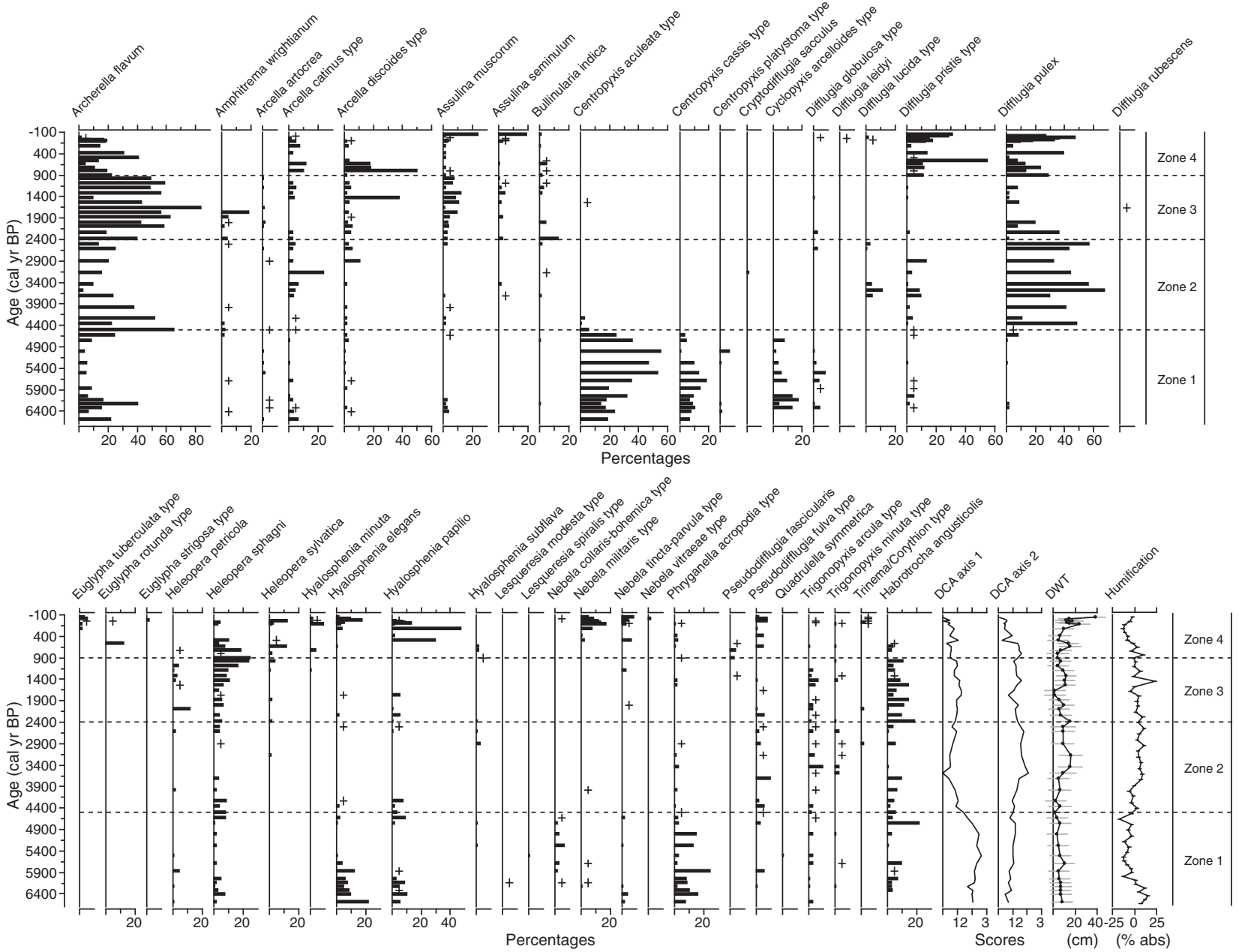

Figure 4. Testate amoebae (TA) from core VC04-06, Hudson Bay Lowlands, northern Ontario, Canada. Zones were derived using constrained cluster analysis (CONISS). Plus signs (+) indicate testate amoeba abundances ≤1%.

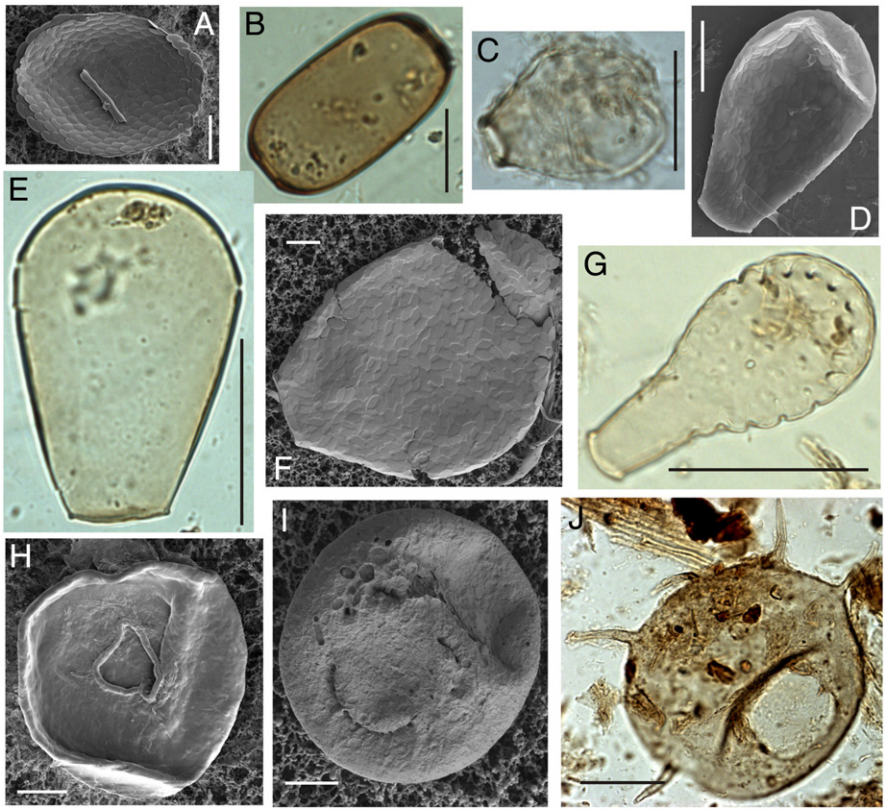

Figure 5. Scanning electron and light micrographs of fossil taxa encountered in core VC04-06, Hudson Bay Lowlands, northern Ontario, Canada. A. *Assulina muscorum*, B. *Archerella flavum*, C. *Difflugia pulex*, D. *Nebela militaris* type, E. *Hyalosphenia papilio*, F. *Nebela tincta-parvula* type, G. *Hyalosphenia elegans*, H. *Trigonopyxis arcula*, I. *Bullinularia indica*, J. *Centropyxis aculeata* type. Scale bars on E, G and J are 50 μm, all others are 20 μm.

Zone 3 —2400 to 900 cal yr BP

An increase in *Assulina muscorum*, *Assulina seminulum*, *H. angusticollis* and *H. sphagni* occurred at the beginning of Zone 3. *A. flavum* continued to dominate (up to 84%) as *Difflugia* spp. declined. DCA axis 1 scores remained constant during this zone, whereas scores on DCA axis 2 were more variable, corresponding to the variations in DWT estimates (min = ~1.6 cm; max = 15.5 cm; average SE = ±9.5 cm). Humification values remained fairly constant.

Zone 4 — 900 cal yr BP to present

Abundances of *D. pulex* recovered in this zone and *D. pristis* became abundant for the first time in the record. *A. flavum* was still an important component of the assemblage although it had declined relative to the previous zone. *Arcella discoides* type and *H. sphagni* were more abundant prior to ~500 cal yr BP, whereas *Hyalosphenia papilio* was more abundant after ~500 cal yr BP, and *Hyalosphenia elegans*, *Nebela militaris* type, and *Assulina* spp. increased following ~100 cal

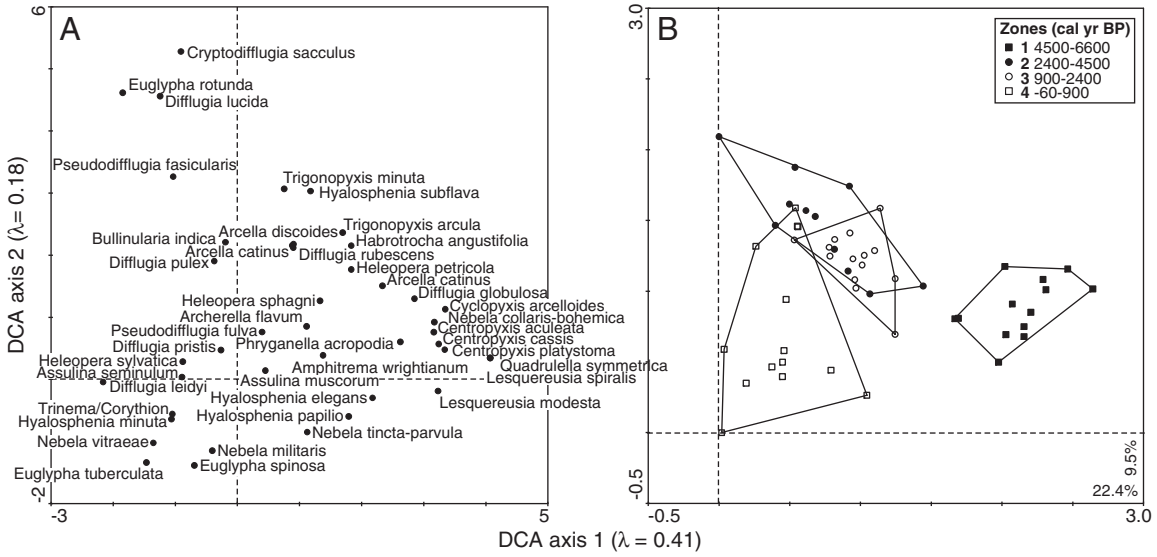

Figure 6. Detrended correspondence analysis (DCA) biplot of A. 43 testate amoeba taxa from B. 52 samples in core VC04-06, Hudson Bay Lowlands, northern Ontario, Canada. Convex hulls are around samples located in the different testate amoeba zones.

https://doi.org/10.1016/j.yqres.2012.05.013 Published online by Cambridge University Press

Table 4
Performance statistics of the modern training set determined using the Modern Analogue Technique (MAT) for mean summer air temperature (June, July and August; TJJA), and total annual precipitation (ANNP). RMSEP = root mean square error of prediction. Sites from the Modern Pollen Database (Whitmore et al., 2005) with pollen sums >300 grains were used to derive our modern training set that consisted of 1983 sites (lake environments only).

Variable	$r^2_{(boot)}$	Max bias$_{(boot)}$	RMSEP
TJJA (°C)	0.94	2.43	1.53
ANNP (mm)	0.76	1795	243

yr BP corresponding with a decline in *A. flavum*. Scores on DCA axes 1 and 2 were lower, as were measurements of peat humification, however DWT values displayed an increasing, yet variable trend with estimates between 4.5 and 15 cm (±9.8 cm).

R Lake — pollen-inferred regional climate reconstructions

The R Lake pollen record (McAndrews et al., 1982) was chosen for paleoclimate reconstructions because of the more regional climate signal that can be obtained from lake sediments, relative to the more local signal recorded in peat core pollen records (Faegri and Iversen, 1989), and the fact that this is the only lake in the region for which pollen data are available. Models of mean summer air temperature (June, July and August; TJJA) and total annual precipitation (ANNP) were developed using a subset of modern pollen assemblages extracted from the dataset of Whitmore et al. (2005), and applied to the fossil pollen record from R Lake (McAndrews et al., 1982). Performance statistics generated using the modern training set show that the predictive ability of the two models is better for temperature than precipitation, however both are reasonably high as indicated by the $r^2_{(boot)}$ (Table 4). This statistic represents the strength of the relationship between the observed and predicted values and can be used to compare models that reconstruct different environmental variables (Birks, 1998). The maximum biases (max bias $_{(boot)}$) are high for both models due to the large size of our training set (1983 sites), which contains a wide range of temperature and precipitation values. However, the low dissimilarity values (SCD) between the modern and fossil samples suggest that these reconstructions are reliable (Fig. 7).

The pollen-based reconstructions indicate that there were no major changes in temperature during the period of record, although the data suggest the possibility of somewhat warmer temperatures up to 4400 cal yr BP and again between 2900 and 2000 cal yr BP, with cooler temperatures from 4400 to 3000 cal yr BP 2000 to 900 cal yr BP. Precipitation exhibited a variable, but somewhat declining trend up to 2200 cal yr BP, after which values increased (Fig. 7). McAndrews et al. (1982) made qualitative interpretations from this palynological record including the possibility that maximum Holocene temperatures occurred from 6500 to 3000 cal yr BP, and Neoglacial cooling took place after 2000 cal yr BP, although it should be noted that the dating of the R Lake core was done at relatively low resolution (two bulk ^{14}C dates and the date of core collection; McAndrews et al., 1982).

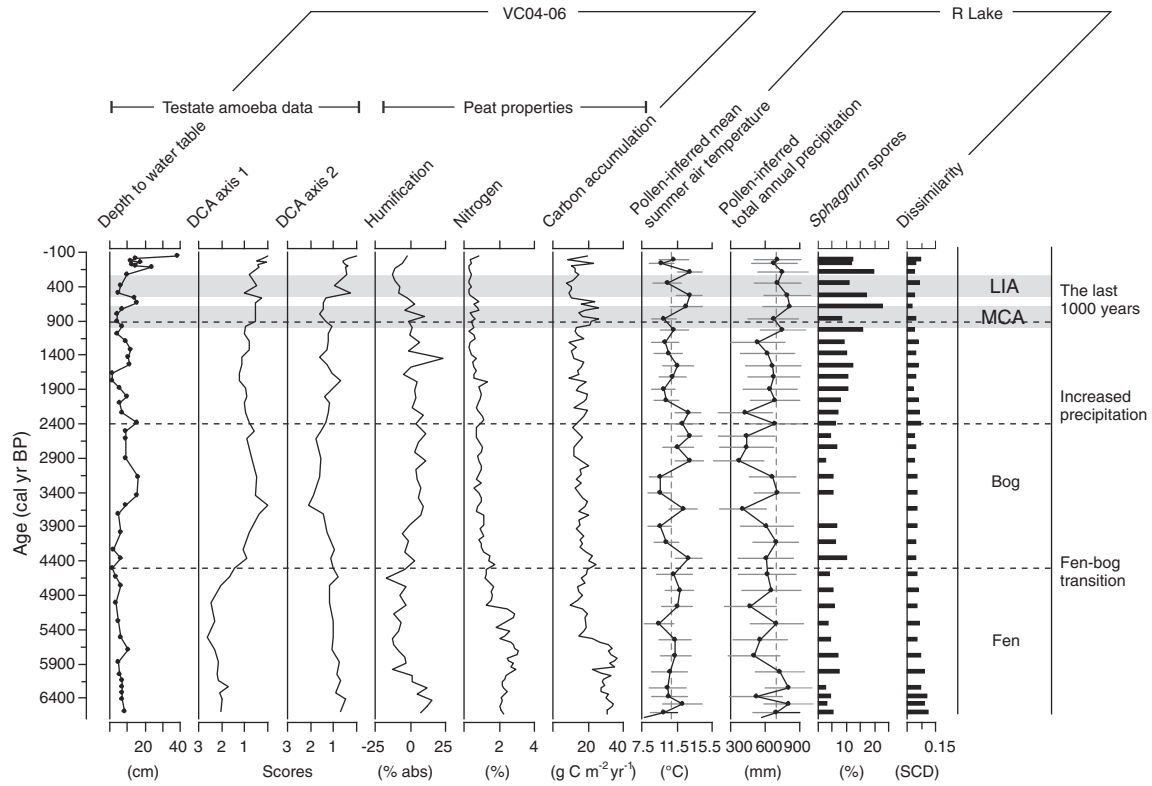

Figure 7. Testate amoeba-inferred water-table depths (DWT), detrended correspondence analysis (DCA) sample scores on axes 1 and 2, detrended humification values, percent nitrogen, and carbon accumulation estimates from core VC04-06. Also shown are pollen-inferred mean summer air temperature (TJJA) and total annual precipitation (ANNP), *Sphagnum* spore abundance, and squared chord distance (SCD) dissimilarity measure between the fossil and the modern samples used to derive the pollen-inferred estimates from R Lake, Hudson Bay Lowlands, northern Ontario, Canada (McAndrews et al., 1982). DWT were estimated using weighted-averaging and a modern testate amoeba training set from Booth (2008), whereas TJJA and ANNP were estimated using the modern analogue technique (MAT) and a modern pollen database from Whitmore et al. (2005). The vertical dashed lines on the paleoclimate estimates indicate the present-day values of TJJA (10.8°C), and ANNP (700 mm), the gray areas represent the timing of the Medieval Climate Anomaly (MCA) and the Little Ice Age (LIA), defined after Mann et al. (2009), and horizontal dashed lines represent the zones determined by the testate amoeba assemblages shown in Figure 4. Note varying scales.

https://doi.org/10.1016/j.yqres.2012.05.013 Published online by Cambridge University Press

Discussion

Carbon accumulation over the past 6700 years

The long-term apparent rates of carbon accumulation (LORCA) during the mid- to late-Holocene was calculated using the core length, the age-depth model (Fig. 2), bulk density measurements, and percent C values (Fig. 3). Estimates ranged between 8.1 and 36.7 g C m^{-2} yr^{-1} (mean ± SD = 18.9 ± 7.3 g C m^{-2} yr^{-1}) for core VC04-06 and agree well with average LORCA values from other northern peatlands (15–27 g C m^{-2} yr^{-1}; e.g. Gorham, 1991; Turunen et al., 2002; Loisel and Garneau, 2010; Yu et al., 2010; van Bellen et al., 2011a). Maximum values for carbon accumulation in the core were recorded prior to 5500 cal yr BP (mean ± SD = 30.7 ± 3.6 g C m^{-2} yr^{-1}), after which they declined and remained relatively stable through the record until they increased again, but more subtly (mean ± SD = 20.3 ± 4.8 g C m^{-2} yr^{-1}), between 1000 and 600 cal yr BP, a time period which coincides in part with the Medieval Climate Anomaly (MCA; Mann et al., 2009). Carbon accumulation rates then dropped between 500 and 100 cal yr BP to the lowest values recorded in the record (mean ± SD = 11.0 ± 1.9 g C m^{-2} yr^{-1}). Although this is coincident with the timing of the Little Ice Age (LIA; Mann et al., 2009), this is confounded by the boundary between the acrotelm and the catotelm at 33 cm (corresponding to 520 cal yr BP, according to our age-depth model; Fig. 3). *Sphagnum* in the acrotelm has a lower bulk density, lower carbon content (Beilman et al., 2009) and is less humified, relative to peat in the catotelm, thus the values for carbon accumulation are not directly comparable in the acrotelm versus the catotelm (Rydin and Jeglum, 2006).

Linking carbon accumulation to paleohydrological and paleoclimatic change

The middle Holocene (6700–2400 cal yr BP)

The testate amoebae assemblages, quantitative DWT reconstruction and peat humification record permit some discussion of paleohydrological change as a driver for the record of carbon accumulation discussed above. According to Andrews and Peltier (1989), the VC04-06 study site emerged from the Tyrrell Sea due to ongoing isostatic uplift soon after 7000 cal yr BP, which is corroborated by our basal radiocarbon age of 6700 cal yr BP (Fig. 2, Table 2). Within ~300 yr of emergence, a fen established at the site, as evidenced by maximum values for percent nitrogen (Rydin and Jeglum, 2006), minerotrophic testate amoeba taxa, and testate amoeba-inferred DWT indicating a near-surface water table persisting up to ~4400 cal yr BP (Fig. 7).

Peat humification values were initially higher during the earliest phase of fen development and declined after 5900 cal yr BP, but the variable values for humification within this zone are difficult to interpret as they are likely being primarily driven by vegetation changes associated with succession from a fen to a bog through this time period (Fig. 7; Yeloff and Mauquoy, 2006). Higher percent nitrogen in the peat suggests a *Carex*-dominated vegetation assemblage existed up to ~4900 cal yr BP (Rydin and Jeglum, 2006). Charman (2002) indicates carbon accumulation rates are typically higher during aquatic/fen stages; similarly higher rates are also recorded in the early part of the VC04-06 record (Fig. 7). Further work on macrofossil remains will help corroborate these interpretations.

By 4400 cal yr BP, a new testate amoeba assemblage had been established that is indicative of bog-like conditions. Greater values for reconstructed DWT after ~3400 cal yr BP, increased humification values, and changes in the testate amoeba community composition (DCA axes 1 and 2 driven primarily by the decline in the wet-indicator taxon *A. flavum*; Fig. 4) suggest a lower water-table position, while bulk density and carbon accumulation do not change appreciably.

An important consideration in this region is the effect of isostatic rebound on hydrology. The early to middle Holocene (8000–7000 cal yr BP) was characterized by very rapid uplift rates to the north of our region (5.5–8 cm yr^{-1}), whereas following 4000 cal yr BP, these rates declined to ~2.7 cm yr^{-1}, and for the past 1000 yr, the rate has been ~1 cm yr^{-1} (Andrews and Peltier, 1989). The influence of glacial isostasy in the middle Holocene in the HBL has been shown to be a major driver of drainage pattern establishment, water-table position and peatland development based on a study from Oldman, Albany and Belec bogs (Fig. 1; Glaser et al., 2004). Although difficult to separate from peatland successional processes, rapid ongoing uplift following land emergence at our site after 6700 cal yr BP may have facilitated a drop in water-table as modulated by drainage changes, contributing to a shift in peatland vegetation, and testate amoeba assemblages indicative of bog-like conditions, which had become established by 4400 cal yr BP.

The late Holocene (2400 cal yr BP to present)

Following the establishment of a bog at the site of VC04-06, the organism community and other variables remained fairly constant until further shifts took place around 2400 cal yr BP. The DWT reconstruction indicates that the water table was generally closer to the surface after 2400 cal yr BP. The slowing rates of isostatic rebound suggest that other explanations, such as climate, should also be considered to explain these changes in the assemblages and inferred surface moisture conditions. Information on regional paleoclimate is given by the R Lake pollen record (Fig. 7). Increasingly wet conditions are coincident with variations in the testate amoeba community on DCA axis 2 and also the DWT estimates. In addition, the increased abundance of *Sphagnum* spores at R Lake over the past 1000 years may reflect paludification driven by wetter conditions (Fig. 7; McAndrews et al., 1982). These combined lines of evidence suggest an increase in precipitation and/or surface moisture conditions through this time, however carbon accumulation remained unchanged. It is possible that the potential for enhanced carbon accumulation through a higher water-table was offset by the cooler temperatures and associated decline in biological productivity associated with Neoglacial cooling (van Bellen et al., 2011b). Evidence in support of this cooling is suggested by the lower pollen-inferred mean summer temperatures up to 900 cal yr BP and from the qualitative consideration of changes in plant taxa observed in the R Lake and Kinosheo Lake Bog palynological records (Kettles et al., 2000; McAndrews et al., 1982).

Despite a probable increase in precipitation after 2400 cal yr BP and cooler temperatures, little change is observed in carbon accumulation until later, around the Medieval Climatic Anomaly (MCA) when surface moisture conditions were wetter, as indicated by the reconstructed DWT estimates (Fig. 7). Temperatures during this time are unclear, as the only available regional paleo-temperature record for our area (R Lake) has coarse sampling resolution since 900 cal yr BP (only six data points) and limited chronological control, both of which restrict us from inferring temperatures during the MCA. Our noted increase in carbon accumulation might itself be a better indicator for regional warming, a conclusion that is further supported by a decline in carbon accumulation recorded in the VC04-06 core at the time of the Little Ice Age (LIA; Fig. 7). However, this finding should be interpreted with caution given the location of the acrotelm–catotelm boundary in the record at 33 cm/~520 cal yr BP (Fig. 3); in the acrotelm, bulk densities are lower thus calculated rates of carbon accumulation are lower independent of climate or other external driver. In the Eastmain River watershed in eastern James Bay (Fig. 1) reduced carbon accumulation corresponded with drier conditions during the LIA (Loisel and Garneau, 2010; van Bellen et al., 2011b). Wetter conditions have been reported from two bogs in northwest Europe (e.g. Mauquoy et al., 2002), and correspond to the findings presented here during this time period from the perspectives of both the DWT estimates and the R Lake record.

Our DWT values are derived from testate amoebae in *Sphagnum*-dominated peatlands between 43° and 47°N (Booth, 2008) that are located 800 km or more to the south of the HBL. Testate amoebae are cosmopolitan organisms, however information regarding their

https://doi.org/10.1016/j.yqres.2012.05.013 Published online by Cambridge University Press

distribution in the HBL is unknown, and a modern calibration set is currently being developed from the western James Bay region that may result in new information regarding the ecological tolerances of certain taxa, and a modified DWT reconstruction. Nevertheless, the DWT reconstruction presented here provides the first quantitative record of surface moisture conditions from Ontario's HBL.

Acknowledgments

Funding for this research was provided by the Ontario Ministry of Natural Resources (OMNR) to Finkelstein, Natural Sciences and Engineering Research Council of Canada and Canadian Foundation for Innovation grants to Finkelstein and Bollmann, and a post-doctoral fellowship from the Centre for Global Change Science at the University of Toronto to Bunbury. We are thankful to J. McLaughlin and B. Hamel from the OMNR for helpful discussions, project support, core collection and a thorough site description, to G. Jeon for providing assistance in the lab, to A. Beaudoin, M. Garneau and K. Gajewski for discussions regarding conifer needles, and especially to R. Booth for assistance regarding testate amoeba identifications and performing the depth to water-table reconstructions.

References

Ali, A.A., Ghaleb, B., Garneau, M., Asnong, H., Loisel, J., 2008. Recent peat accumulation rates in minerotrophic peatlands of the Bay James region, Eastern Canada, inferred by Pb-210 and Cs-137 radiometric techniques. Applied Radiation and Isotopes 66, 1350–1358.

Andrews, J.T., Peltier, W.R., 1989. Quaternary geodynamics of Canada. In: Fulton, R.J. (Ed.), Quaternary Geology of Canada and Greenland. Geological Survey of Canada, pp. 543–572.

Beilman, D.W., MacDonald, G.M., Smith, L.C., Reimer, P.J., 2009. Carbon accumulation in peatlands of West Siberia over the last 2000 years. Global Biogeochemical Cycles 23, GB1012. http://dx.doi.org/10.1029/2007GB003112.

Bennett, K.D., 1996. Determination of the number of zones in a biostratigraphical sequence. The New Phytologist 132, 155–170.

Birks, H.J.B., 1998. Numerical tools in palaeolimnology — progress, potentialities, and problems. Journal of Paleolimnology 20, 307–332.

Blaauw, M., 2010. Methods and code for "classical" age-modelling of radiocarbon sequences. Quaternary Geochronology 5, 512–518.

Blackford, J.J., Chambers, F.M., 1993. Determining the degree of peat decomposition for peat-based palaeoclimatic studies. International Peat Journal 5, 7–24.

Booth, R.K., 2008. Testate amoebae as proxies for mean annual water-table depth in *Sphagnum*-dominated peatlands of North America. Journal of Quaternary Science 23, 43–57.

Charman, D.J., 2001. Biostratigraphic and palaeoenvironmental applications of testate amoebae. Quaternary Science Reviews 20, 1753–1764.

Charman, D., 2002. Peatlands and Environmental Change. John Wiley & Sons Ltd., West Sussex, England.

Charman, D.J., Hendon, D., Woodland, W.A., 2000. The identification of testate amoebae (Protozoa: Rhizopoda) in peats. Technical Guide No. 9. Quaternary Research Association, London.

de Jong, R., Blaauw, M., Chambers, F.M., Christensen, T.R., de Vleeschouwer, F., Finsinger, W., Fronzek, S., Johansson, M., Kokfelt, U., Lamentowicz, M., Le Roux, G., Mauquoy, D., Mitchell, E.A.D., Nichols, J.E., Samaritani, E., van Geel, B., 2010. Climate and peatlands. In: Dodson, J. (Ed.), Changing Climates, Earth Systems and Society. Springer, New York, pp. 85–121.

Dyke, A.S., Prest, V.K., 1987. Paleogeography of northern North America, 18 000–5 000 years ago. Geological Survey of Canada.

Environment Canada, 2000. Canadian climate normals. Environment Canada, Ottawa. Available at http://www.climate.weatheroffice.gc.ca/climate_normals/.

Faegri, K., Iversen, J., 1989. Textbook of Pollen Analysis. John Wiley & Sons, Toronto.

Far North Science Advisory Panel, 2010. Science for a Changing North: Report to the Ontario Ministry of Natural Resources. The Queen's Printer for Ontario, Toronto.

Frolking, S., Roulet, N.T., 2007. Holocene radiative forcing impact of northern peatland carbon accumulation and methane emissions. Global Change Biology 13, 1079–1088.

Fulton, R.J., 1995. Surficial materials of Canada. Map 1880A. (Compiler) Geological Survey of Canada, Ottawa.

Gagnon, A.S., Gough, W.A., 2005. Climate change scenarios for the Hudson Bay region: an intermodel comparison. Climatic Change 69, 269–297.

Glaser, P.H., Siegel, D.I., Reeve, A.S., Janssens, J.A., Janecky, D.R., 2004. Tectonic drivers for vegetation patterning and landscape evolution in the Albany River region of the Hudson Bay Lowlands. Journal of Ecology 92, 1054–1070.

Gorham, E., 1991. Northern peatlands: role in the carbon cycles and probable responses to climatic warming. Ecological Applications 1, 182–195.

Grimm, E.C., 1987. CONISS: A FORTRAN 77 program for stratigraphically constrained cluster analysis by the method of incremental sum of squares. Computers & Geosciences 13, 13–35.

Juggins, S., 2003. C^2 user guide. Software for ecological and palaeoecological data analysis and visualisation. Newcastle upon Tyne. University of Newcastle, UK.

Juggins, S., 2009. Rioja: an R Package for the Analysis of Quaternary Science Data, Version 0.5-6.

Kettles, I.M., Garneau, M., Jetté, H., 2000. Macrofossil, pollen, and geochemical records of peatlands in the Kinosheo Lake and Detour Lake areas, northern Ontario. Bulletin, 545. Geological Survey of Canada, Ottawa.

Kleinen, T., Brovkin, V., von Bloh, W., Archer, D., Munhoven, G., 2010. Holocene carbon cycle dynamics. Geophysical Research Letters 37, L02705.

Loisel, J., Garneau, M., 2010. Late Holocene paleoecohydrology and carbon accumulation estimates from two boreal peat bogs in eastern Canada: potential and limits of multi-proxy archives. Palaeogeography, Palaeoclimatology, Palaeoecology 291, 493–533.

MacDonald, G.M., Beilman, D.W., Kremenetski, K.V., Sheng, Y.W.S.L.C., Velichko, A.A., 2006. Rapid early development of circumarctic peatlands and atmospheric CH_4 and CO_2 variations. Science 314, 285–288.

Mann, M.E., Zhang, Z., Rutherford, S., Bradley, R.S., Hughes, M.K., Shindell, D., Ammann, C., Faluvegi, G., Fenbiao, N., 2009. Global signatures and dynamical origins of the Little Ice Age and Medieval Climate Anomaly. Science 326, 1256–1260.

Martini, I.P., 2006. The cold-climate peatlands of the Hudson Bay Lowland, Canada: brief overview of recent work. In: Martini, I.P., Martinez Cortizas, A., Chesworth, W. (Eds.), Peatlands: Evolution and Records of Environmental and Climate Change. Elsevier, pp. 53–83.

Mauquoy, D., Engelkes, T., Groot, M.H.M., Markesteijn, F., Oudejans, M.G., van der Plicht, J., van Geel, B., 2002. High-resolution records of late-Holocene climate change and carbon accumulation in two north-west European ombrotrophic peat bogs. Palaeogeography, Palaeoclimatology, Palaeoecology 186, 275–310.

McAndrews, J.H., Riley, J.L., Davis, A.M., 1982. Vegetation history of the Hudson Bay Lowland: a postglacial pollen diagram from the Sutton Ridge. Le Naturaliste Canadien 109, 597–608.

National Atlas Information Service, 1995. Canada, permafrost. Map MCR4177. Natural Resources Canada, Ottawa.

Overpeck, J.T., Webb III, T., Prentice, I.C., 1985. Quantitative interpretation of fossil pollen spectra: dissimilarity coefficients and the method of modern analogs. Quaternary Research 23, 87–108.

Payne, R.J., Mitchell, E.A.D., 2009. How many is enough? Determining optimal count totals for ecological and palaeoecological studies of testate amoebae. Journal of Paleolimnology 42, 483–495.

R Development Core Team, 2011. R: A Language and Environment for Statistical Computing (version 2.13.2). R Foundation for Statistical Computing, Vienna, Austria.

Reimer, P.J., Baillie, M.G.L., Bard, E., Bayliss, A., Beck, J.W., Blackwell, P.G., Bronk Ramsey, C., Buck, C.E., Burr, G.S., Edwards, R.L., Friedrich, M., Grootes, P.M., Guilderson, T.P., Hajdas, I., Heaton, T.J., Hogg, A.G., Hughen, K.A., Kaiser, K.F., Kromer, B., McCormac, F.G., Manning, S.W., Reimer, R.W., Richards, D.A., Southon, J.R., Talamo, S., Turney, C.S.M., van der Plicht, J., Weyhenmeyer, C.E., 2009. IntCal09 and Marine09 radiocarbon age calibration curves, 0–50,000 years cal BP. Radiocarbon 51, 1111–1150.

Riley, J.L., 2003. Flora of the Hudson Bay Lowland and its postglacial origins. National Research Council of Canada, Ottawa.

Riley, J.L., 2011. Wetlands of the Hudson Bay Lowland: An Ontario Overview. Nature Conservancy of Canada, Toronto.

Rydin, H., Jeglum, J., 2006. The Biology of Peatlands. Oxford University Press, Oxford.

ter Braak, C.J.F., Šmilauer, P., 2002. CANOCO for Windows: Software for Community Ordination (version 4.5). Microcomputer Power, Ithaca, New York.

Turunen, J., Tomppo, E., Tolonen, K., Reinikainen, A., 2002. Estimating carbon accumulation rates of undrained mires in Finland — application to boreal and subarctic regions. The Holocene 12, 69–80.

van Bellen, S., Dallaire, P.-L., Garneau, M., Bergeron, Y., 2011a. Quantifying spatial and temporal Holocene carbon accumulation in ombrotrophic peatlands of the Eastmain region, Quebec, Canada. Global Biogeochemical Cycles 25, GB2016. http://dx.doi.org/10.1029/2010GB003877.

van Bellen, S., Garneau, M., Booth, R.K., 2011b. Holocene carbon accumulation rates from three ombrotrophic peatlands in boreal Quebec, Canada: impact of climate-driven ecohydrological change. The Holocene 21, 1217–1231.

Wania, R., Ross, I., Prentice, I.C., 2009. Integrating peatlands and permafrost into a dynamic global vegetation model: 2. Evaluation and sensitivity of vegetation and carbon cycle processes. Global Biogeochemical Cycles 23, GB3015. http://dx.doi.org/10.1029/2008GB003413.

Wheeler, J.O., Hoffman, P.F., Card, K.D., Davidson, A., Sandford, B.V., Okulitch, A.V., Roest, W.R., 1997. Geological map of Canada. Map D1860A. (Compilers) Geological Survey of Canada, Ottawa.

Whitmore, J., Gajewski, K., Sawada, M., Williams, J.W., Minckley, T., Shuman, B., Bartlein, P.J., Webb III, T., Viau, A.E., Shafer, S., Anderson, P., Brubaker, L.B., 2005. A North American modern pollen database for multi-scale paleoecological and paleoclimatic applications. Quaternary Science Reviews 24, 1828–1848.

Williams, J.W., Shuman, B., 2008. Obtaining accurate and precise environmental reconstructions from the modern analog technique and North American surface pollen dataset. Quaternary Science Reviews 27, 669–687.

Yeloff, D., Mauquoy, D., 2006. The influence of vegetation composition on peat humification: implications for palaeoclimatic studies. Boreas 35, 662–673.

Yu, Z.C., Campbell, I.D., Campbell, C., Vitt, D.H., Bond, G.C., Apps, M.J., 2003. Carbon sequestration in western Canadian peat highly sensitive to Holocene wet-dry climate cycles at millenial timescales. The Holocene 13, 801–808.

Yu, Z.C., Loisel, J., Brosseau, D.P., Beilman, D.W., Hunt, S.J., 2010. Global peatland dynamics since the Last Glacial Maximum. Geophysical Research Letters 37, GL043584. http://dx.doi.org/10.1029/2010GL043584.